Journal of Mathematical Chemistry 10(1992)249–274

A THEORETICAL ANALYSIS OF EXCITED STATE PROTON TRANSFER IN 3-HYDROXYFLAVONE. PROMOTING EFFECT OF A LOW FREQUENCY BENDING MODE

Andrea PELUSO, Carlo ADAMO and Giuseppe DEL RE
Cattedra di Chimica Teorica, Università Federico II di Napoli, via Mezzocannone 4, 80134 Napoli, Italy

Abstract

The dynamical properties of excited state intramolecular proton transfer in 3-hydroxyflavone have been analyzed on the basis of the time evolution of the quantum states of the two isomeric forms. Potential energy surfaces have been computed at the MNDO/AM1 level. The results shed light on the essential features of the proton transfer mechanism: in particular, the rapidity of the process is to be attributed to the promoting effect of a low frequency bending vibration, which shortens the distance between donor and acceptor atoms.

1. Introduction

Hydrogen bonds continue to attract considerable attention because of the important role they play in many processes of biochemical and technological interest. In the last decade, many efforts have been concentrated on the investigation of systems characterized by intramolecular hydrogen bonds: such systems are probably involved in information storage at the molecular level and in photochemical hole burning [1]; the possible involvement of proton tunneling in the primary event of vision has also been suggested [2].

The fluorescence spectra of molecules with intramolecular H-bonds are usually characterized by very large Stokes shifts, so that the emission bands are not a mirror image of the absorption bands. Weller originally showed that the anomalous emission of methyl salicylate can be quenched by methylation of the acidic proton and suggested that the red-shifted emission takes place from an isomer, formed via excited state intramolecular proton transfer (ESIPT) [3]. The proposed explanation is schematically shown in fig. 1: the most stable position of the hydrogen atom is inverted upon excitation, so that the excited molecule undergoes isomerization to the tautomeric form, followed by fluorescence decay to the ground state with a longer wavelength emission.

The reverse ground-state proton transfer is also energetically favoured, the entire process is cyclic and in most cases efficient. This behaviour was observed in many heteroaromatics possessing a hydroxyl group close to an heteroatom acting as proton acceptor [4–10].

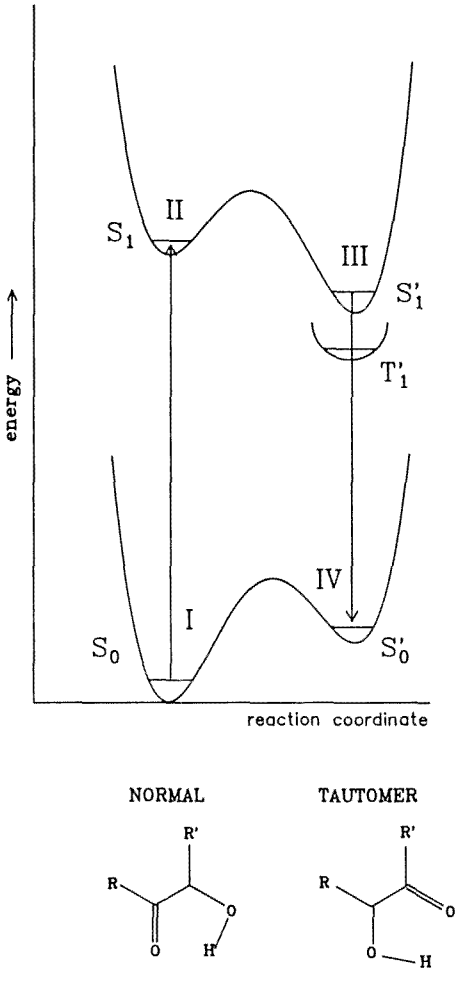

Fig. 1. Qualitative potential energy profiles for excited state intramolecular proton transfer.

The driving force for proton transfer in an excited state is provided by change, upon excitation, of the acid-base properties of donor and/or acceptor group [11]. When ESIPT is fast and irreversible, the molecule can act as an UV stabilizer, especially if the internal conversion decay rate is faster than radiative emission [12]. If the "proton transferred" form has a long lifetime, the system is a potential laser dye, since population inversion can be obtained in a few picoseconds [13].

This paper is intended as a theoretical contribution to the understanding of the structural features which determine the spectral behaviour just mentioned. We have studied in particular the case of 3-hydroxyflavone (3-HF).

The 3-HF molecule, the basic component of natural pigments contained in plant leaves with the probable function of UV protector [14], is a much studied

ESIPT system. The interest aroused by 3-HF is due to the complex behaviour of its ESIPT dynamics; the main features of the process, namely the strong dependence of ESIPT rate on temperature and environmental effects, are still a matter of debate.

The steady-state photoluminiscence spectrum of 3-HF [15–20] is characterized by an absorption band starting at 370 nm, with the first peak at 350 nm. At room temperature, the fluorescence spectrum shows only one emission band, with a peak at approximately 530 nm, but on cooling at 77 K a second emission appears in the blue region around 410 nm. The dual emission of 3-HF has been interpreted by Sengupta and Kasha [15] in terms of two stable excited state structures, the 4-keto form (usually called normal form), which emits at 410 nm, and the 3-keto form (tautomer)*, originating from the intramolecular proton transfer:

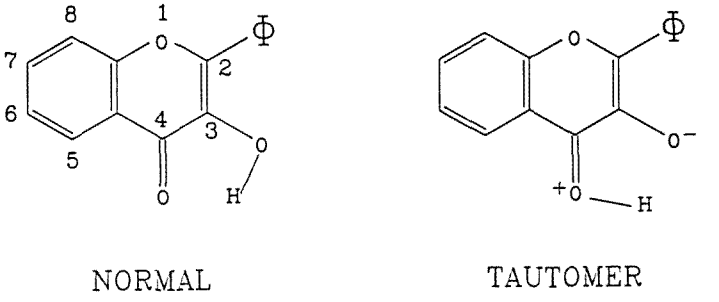

NORMAL TAUTOMER

Scheme 1.

The very strong temperature dependence of the emission spectrum has been tentatively explained in terms of an energy barrier to proton transfer, whose height depends on the viscosity of the medium. This behaviour may be understood by considering that the motion of the proton and the phenyl torsional mode are strongly coupled, as can be inferred from the fact that the tautomeric form is resonance stabilized for a coplanar position of the phenyl ring. However, Woolfe and Thistlethwaite [16] showed that at room temperature the emission band of the normal form is not present, even if the rigidity of the medium is strongly increased. Therefore, they ascribed the dramatic change in the fluorescence spectrum solely to the effect of temperature on excited state processes in 3-HF.

A strong solvent dependence of the emission spectrum was also detected [16]: normal emission is always observed in solvents with hydrogen bond capability, even at room temperature, and the band at longer wavelength is considerably less intense than in hydrocarbon solvents. On the contrary, in highly purified and extremely dry hydrocarbon solvents, the emission band of the normal form does not appear,

*We will hereafter refer to the 4-keto and 3-keto forms as normal and tautomer, respectively; this is probably not the most correct terminology since, as one referee noted, the two forms are tautomers of each other; however, it is in line with the pre-existing literature on the subject.

regardless of temperature and viscosity [18]. These observations have led to the conclusion that the long, intramolecular hydrogen bond, which is bent and hence weak [21,22], is disrupted and replaced by stronger, linear, intermolecular hydrogen bonds with solvent molecules or impurities capable of forming hydrogen bonds.

Further insight into the kinetics of ESIPT isomerization and its dependence on solvent, temperature and molecular substitutions has been obtained by picosecond resolved spectroscopy. Itoh et al. [23] compared time resolved spectra of 3-HF with those of 3-hydroxychromone (3-HC), which differs from 3-HF only by the absence of the phenyl group on the gamma-pyrone ring. While in 3-HC ESIPT is unresolvably fast, 3-HF shows a detectable fluorescence rise time, thus confirming the role of the phenyl ring.

Strandjord et al. [24] found two components of the rise time of the tautomer fluorescence at room temperature. They suggested that the faster component originates by the ESIPT taking place from a highly excited vibrational state initially populated by photo-excitation, while the slower component originates from a proton transfer occurring after vibrational relaxation [24,25].

The temperature dependence of the rise time of the tautomer fluorescence has been studied by McMorrow et al. [26]. They have reported a rise time of less than 8 ps at 298 K, increasing to 40 ps at 77 K.

All these experiments indicate the existence of an intrinsic, though small, energy barrier to ESIPT. However, studies in an argon matrix in conditions which should prevent the formation of hydrogen bonds with water impurities showed that ESIPT in 3-HF is very fast, even at very low temperature (10–15 K) [27–29]. The measured tautomer fluorescence rise time is approximately 3 ps, implying a rate constant for the ESIPT process $K \geq 10^{12}$ s^{-1}. It is noteworthy that in the experiments of Dick and Ernsting [28], an excitation source of 308 nm has been used, so that highly excited vibrational states are probably populated by the photoexcitation, while Brucker and Kelley [27], who used an excitation source at 354 nm, also reported evidence, from the excitation spectra of the normal and deuterated molecule, in favour of an intrinsic barrier to proton transfer. According to more recent results, it appears that ESIPT in 3-HF is a very fast process, at least for the bare molecule. However, the physical reasons of such a behaviour are still unknown. The fact that heteroaromatics change their acid-base properties upon excitation can account for the relative stability of the normal and tautomeric form, but does not explain the absence of an intrinsic barrier to proton transfer in a long H-bridge such as the intramolecular H-bond in 3-HF. Very fast proton transfers, without an intrinsic barrier, are known to occur whenever they prevent the formation of charge separation structures, but this does not seem to be the case of ESIPT in 3-HF. Moreover, there are still uncertainties regarding the role of the phenyl ring and of solvent effects, as inferred by the fact that the longer wavelength emission is still observed in the case in which only one intermolecular H-bond is formed with a solvent molecule [30].

Conflicting views can be found in the literature on most of the above topics, even though no open debate has taken place. Further insight into the nature of the electronic excited states of 3-HF and of the photoisomerization mechanism is therefore desirable and can be obtained by a theoretical analysis centered on the time evolution of the 3-HF quantum states. A previous computation on 3-HF [31] has been devoted to the calculation of vertical transition energies and oscillator strengths. An ab initio RPA computation of the energy barrier to proton transfer has been carried out for the 3-HF [32], but the authors have explored only a few points of the potential energy surfaces. Therefore, we have applied the scheme recently developed in this group [54] to study the temporal aspects of ESIPT in 3-HF, using ad hoc potential energy surfaces. The existence of a barrier to proton transfer and the role of low frequency modes have been assessed. The present analysis also sheds light on the observed temperature and solvent effects.

2. Computational details

All computations have been carried out in the MNDO approximation [33] (AM1 parameterization [34]) supplemented by a CI treatment [35] since, according to the large number of published applications, the MNDO approximation yields reliable results for ground-state geometries and heats of formation, in particular for organic compounds. The large size of the systems and the need of investigating the potential energy surface of electronic excited states for several degrees of freedom, do not allow the use of more sophisticated computational techniques such as ab initio CI or multiconfigurational schemes. This holds especially if one considers that ab initio accurate computations of hydrogen bond energetics require a large basis set, including polarization functions on the atoms involved in the H-bridge [36].

The quality of the MNDO approximation as for excited states is more difficult to assess, since only a few papers have been published on this application [37–42]. If applied with some caution, it should allow the calculation of excited state properties with a reasonable degree of approximation, especially for the ordering of the states and their relative energies on conformational changes. Encouraging results have been obtained in studies of the dynamics of relevant photochemical processes [38, 39] and in the investigation of conformational changes induced in polyenes by photoexcitation [40–41]. In particular, Ertl [42] has noted that AM1, a reparameterized MNDO scheme with modified core–core interaction terms, yields geometrical parameters for excited states in better agreement with experimental results; its only drawback is a slightly too large stabilization of excited states [35], resulting in low transition energies.

On the other hand, MNDO methods fail to describe the energetics of hydrogen bond systems [43]. In particular, the AM1 approximation overestimates hydrogen bond interactions, preferring, whenever possible, bifurcated structures with respect to linear ones. However, in those cases in which bifurcated hydrogen bonds are not

possible, AM1 results are of comparable quality with DZ and DZO ab initio results [44], at least for equilibrium geometry and stabilization energy. With regard to the calculation of energy barrier to proton transfer, a test computation on malonaldehyde [45] suggests that the above quantities are overestimated by a factor of approximately 2 with respect to accurate ab initio computations [51,52]; however, this is not a serious problem for the system under study since, as shown later, the emerging picture may only marginally depend on the accuracy of the computed energy barrier to proton transfer.

In short, computations such as MNDO/AM1 can be expected to provide reliable information on the potential energy surfaces governing the ESIPT process and its dependence on phenyl motion and molecular substitutions. Quantitative reliability cannot be demanded, but this is not a serious drawback in the present state of the art because, as Troe et al. have pointed out, exact quantitative information on such systems is at present not obtainable, either from quantum mechanical calculations or from the experimental determination of the vibrational frequencies of the excited states [37].

The computations have been carried out using the MOPAC 6.0 package of Stewart et al. [46], a version implemented with the analytical first derivative of the CI energy with respect to internal coordinates and thus allowing fast optimization of excited state geometries [47]. The excited states have been computed with the inclusion of configuration interaction (CI); the lowest 100 configurations, obtained by exciting electrons from the three highest occupied to the three lowest empty MOs, have been explicitly included in the CI matrix, whose diagonalization leads to state energies and state vectors. Both singly and doubly excited configurations have been considered. A more extended CI computation, including the fourth occupied and virtual levels, did not substantially change the computed energies of the lower states.

3. Results

3.1. THE ELECTRONIC STATES OF 3-HF

The ground-state geometry of the normal form of 3-HF has been fully optimized with respect to bond distances and valence angles. Distortion from planarity has not been allowed, except for the phenyl group, which we have found to lie 29 degrees off the main molecular plane. With regard to the lowest excited singlets of both forms, only a few geometrical parameters, which are likely to be involved in the relaxation processes following photoexcitation, have been optimized. As Dewar et al. have pointed out [35], highly accurate excited-state geometries cannot be obtained; however, for the system under study, as in previous works [37–42], computed geometries are acceptable, giving a reasonable trend with respect to ground-state geometries. The results of all optimizations performed are presented in fig. 2. (For the sake of completeness, we have also included results for the ground-state geometry which have already been presented by Dick [31].) The computed

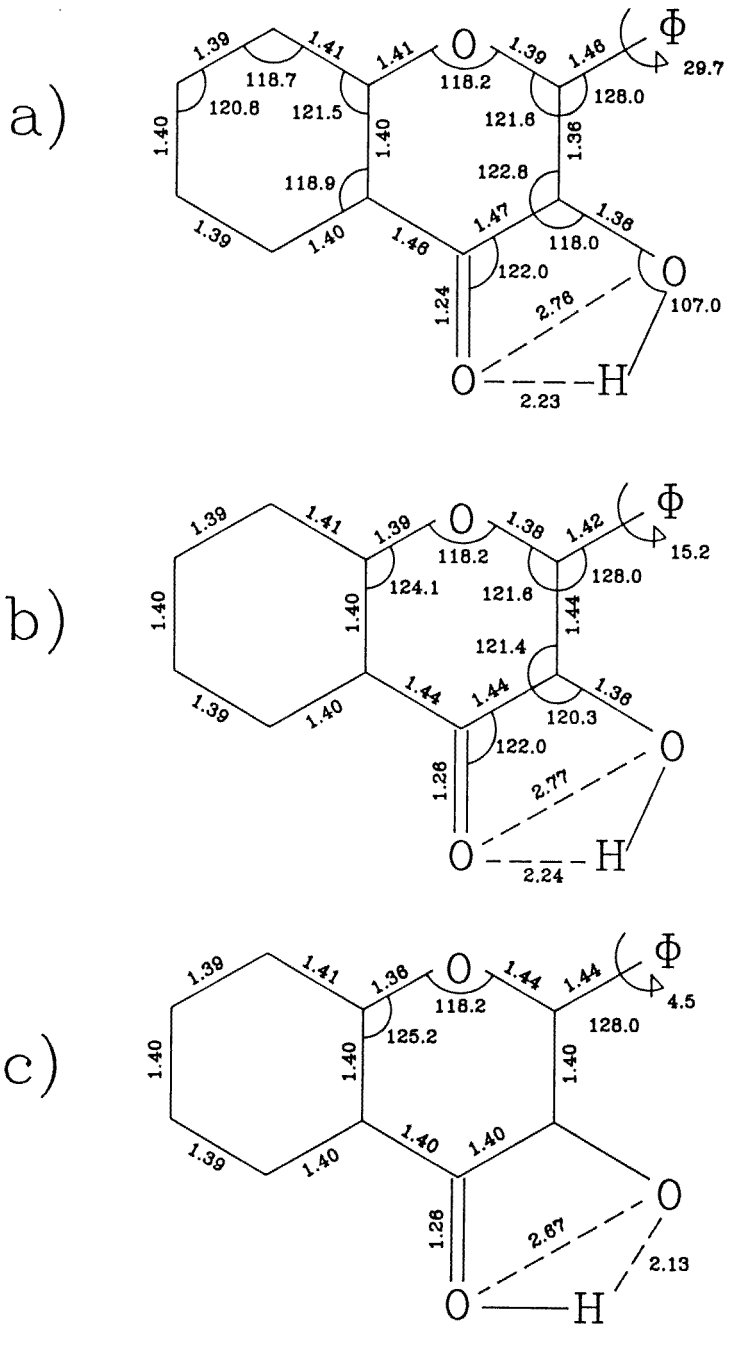

Fig. 2. Optimized geometries of 3-hydroxyflavone: ground state normal form (a), and excited state normal (b) and tautomeric (c) forms.

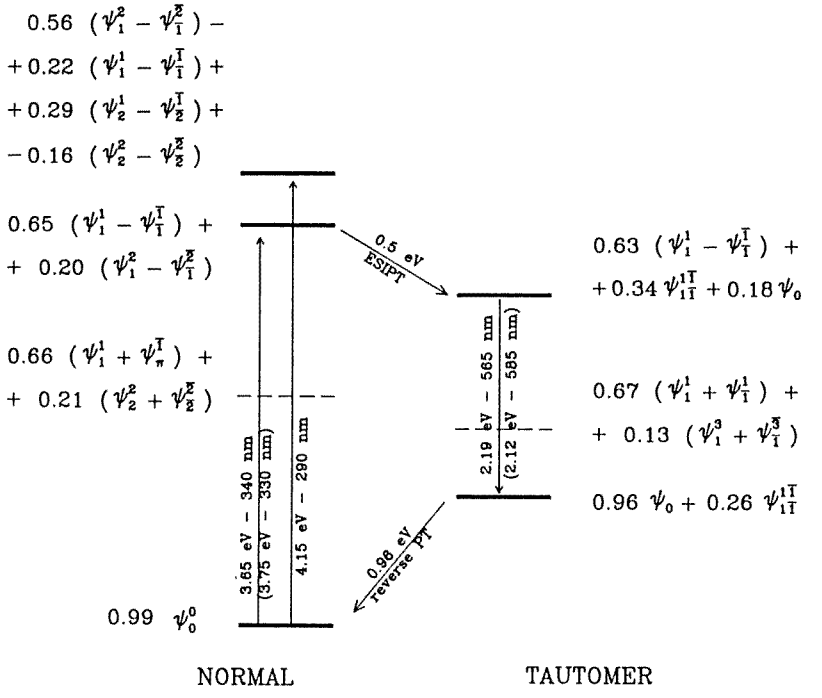

Fig. 3. Computed MNDO/AM1-CI transition energies and schematic state vectors for the lower excited singlets and triplets of 3-HF. The numbering of levels starts from the HOMO for occupied MOs and from the LUMO for the virtual ones. PPP transition energies are reported in parentheses.

state energies of the lowest singlet and triplet states of the normal and tautomeric forms for 3-HF are shown in fig. 3. The energy values refer to Franck–Condon transitions, starting from the optimized geometries of the normal-form ground state and that of the tautomer's first excited singlet. The transition energies are in fairly good agreement with experimental results. The absorption spectrum of 3-HF shows two strong bands with a maximum at approximately 350 and 300 nm [15–20]; the computed MNDO transition energies from the normal ground state to the first two singlets are 3.65 and 4.15 eV, corresponding to a wavelength of 340 and 290 nm, respectively. (The PPP results are also reported in parentheses in fig. 3 for comparison.)

As expected, the first singlet–singlet transitions of the normal and tautomeric forms are of $\pi \rightarrow \pi^*$ type. The first excited state of the normal form corresponds to the HOMO–LUMO excitation with a small contribution of the HOMO–(LUMO + 1); for the tautomer the situation is similar, with small contributions coming from the SCF ground state and the doubly excited HOMO–LUMO configurations. (State vectors are reported in fig. 3.)

In order to understand the electronic features of the first excited singlet and the factors that induce proton transfer, it may be sufficient to focus attention on the

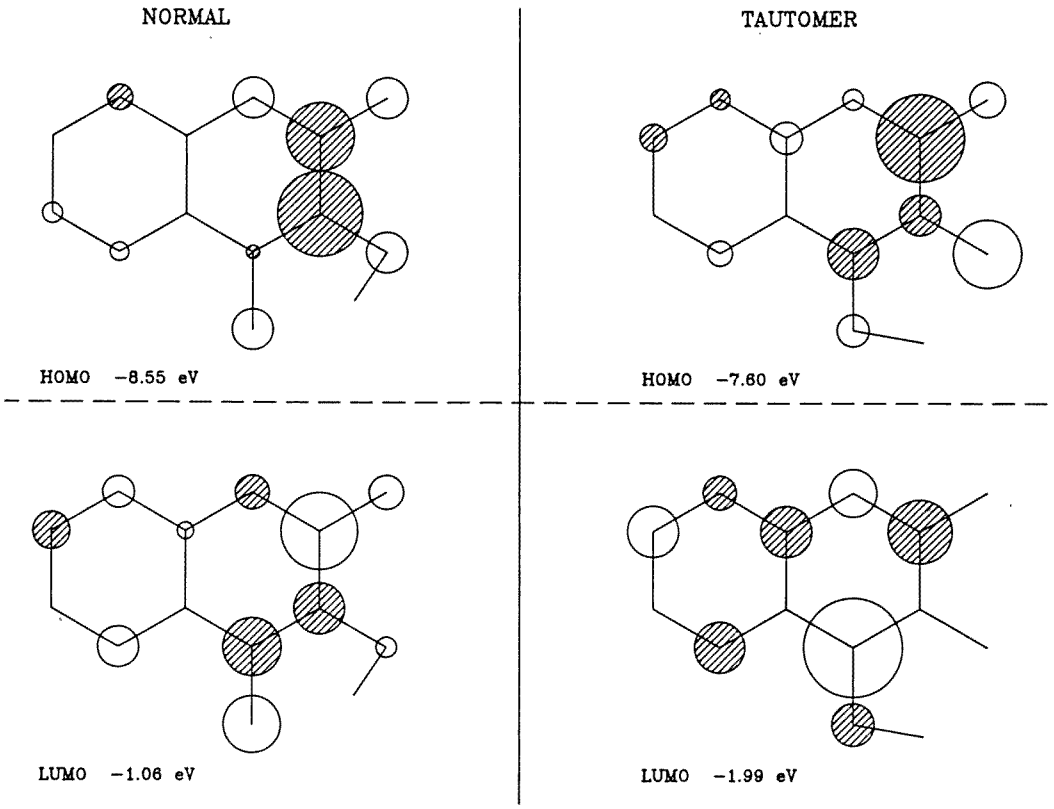

Fig. 4. Schematic plot of the HOMO and LUMO levels of 3-HF. Circle radius is proportional to atomic coefficients.

character of the HOMO and LUMO levels of the two isomeric forms; they are sketched in fig. 4. The HOMO levels of the normal and tautomeric forms are very similar to one another. They correspond mainly to a bonding contribution of the p_z atomic orbitals of the 2nd, 3rd and 4th carbon atoms of the gamma-pyrone ring, with an antibonding interaction with the p_z orbitals of the three oxygen atom and the bonded carbon atom of the phenyl group. The HOMO energy is lower in the normal form, where the C_2-C_3 double bond is formally allowed, while it increases by about 1 eV in the tautomer, where the C_3-O double bond prevents its formation.

On the other hand, the LUMO levels of the two forms are somewhat different: in the normal form there are strong C_2-C_3 and C_4-O antibonding interactions, which disappear in the tautomer where only the π antibonding interaction for the C–O single bond is preserved. Therefore, in the tautomer the LUMO level appears to be mainly a non-bonding level and it is stabilized with respect to its counterpart in the normal form. Thus, the behaviour of the system after photoexcitation can be understood, in a first approximation, using a simple four-level scheme: in the ground state, the HOMO level is stabilized by the hydroxyl group in position 3, while in the excited state, mainly consisting in an excitation of one electron from

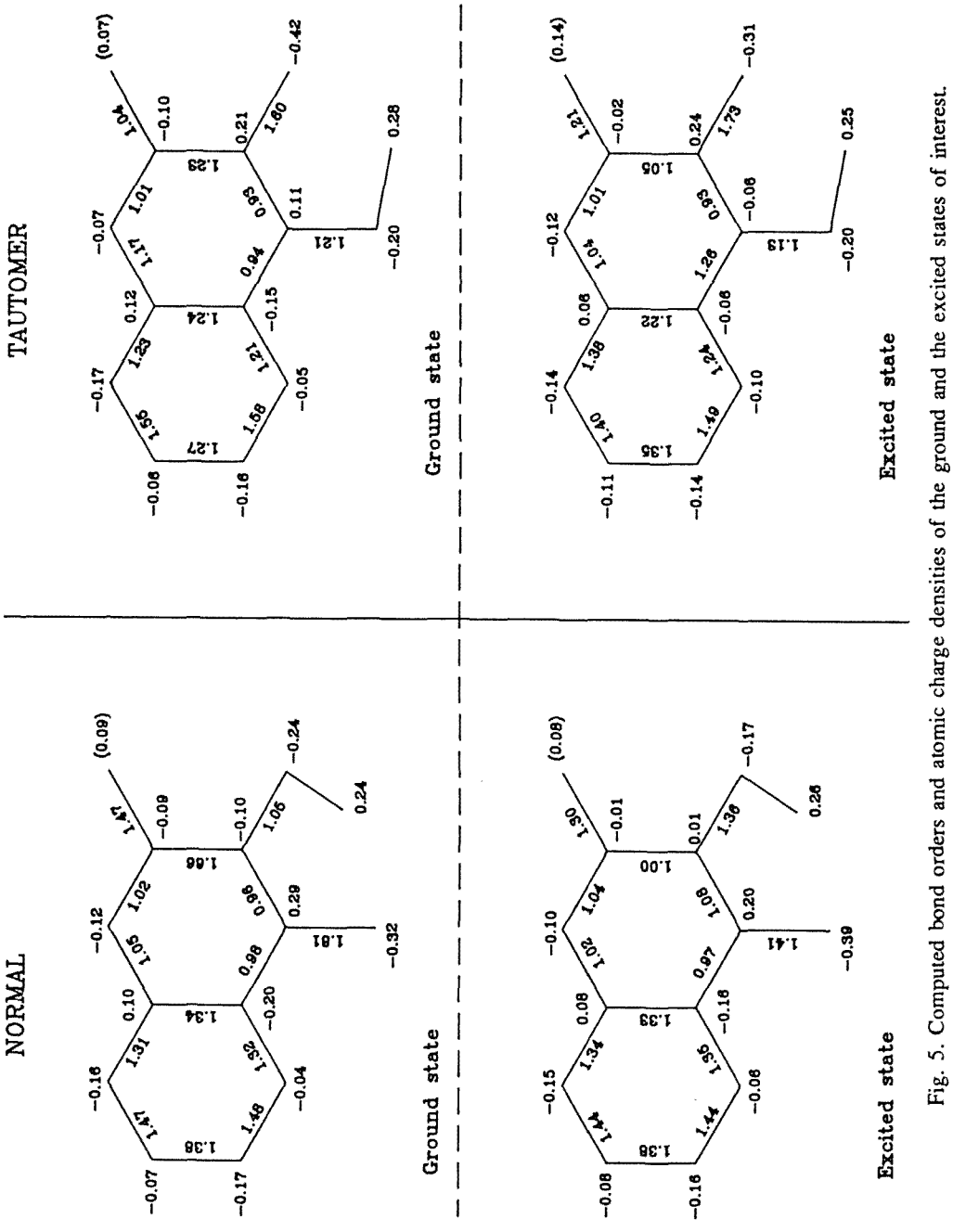

Fig. 5. Computed bond orders and atomic charge densities of the ground and the excited states of interest.

the HOMO to the LUMO levels, the hydroxyl group occupies preferentially the 4th position, stabilizing the LUMO level.

This simple scheme is further supported by considerations based on the computed bond orders and net atomic charges. The latter quantities have been computed at the SCF level, considering that in the excited states the system behaves as a biradical, with two electrons occupying the two lowest accessible levels. Results are shown in fig. 5. The most important changes produced by excitation are the strong decreases in the bond orders of the C_2-C_3 and C_4-O double bonds (1.66 to 1.00 Å and 1.80 to 1.41 Å, respectively), and the corresponding increases of the C_3-O and C_3-C_4 single bonds (1.05 to 1.36 Å and 0.96 to 1.08 Å, respectively). A partial double bond with the phenyl ring is also formed. The situation can be schematically represented as follows:

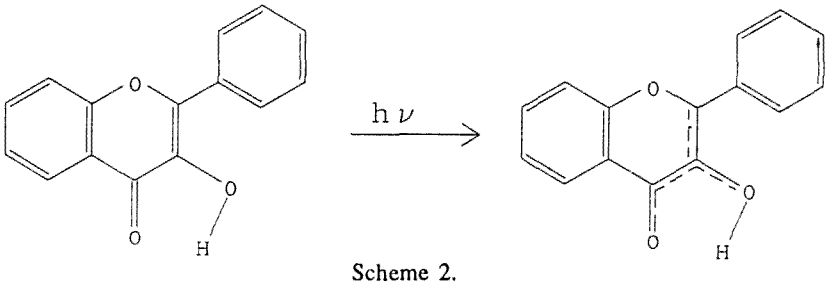

Scheme 2.

confirming that the major effect of photoexcitation is the breaking of the two double bonds of the heteronuclear ring, which are redistributed on both C–O bonds and the adjacent C–C single bond, and on the bond connecting the phenyl ring. Optimized bond distances, shown in fig. 2, follow the same trend. Changes in net atomic charges are more modest. The total atomic charge of the phenyl group remains unchanged, and the only relevant changes are localized on the oxygen atoms and on the carbons bound to them. No evidence of charge separation, which would imply a very fast proton transfer without an intrinsic barrier [48], has been found. As the proton switches to the position characteristic of the tautomeric form, the C–O bond orders revert to a single and double bond, in a situation inverted with respect to the normal form. The following resonance structures appear to be predominant:

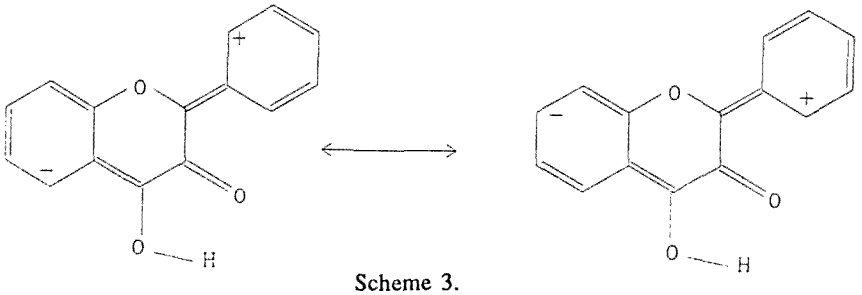

Scheme 3.

as suggested by several factors: the higher negative charge on the 5th and 7th carbon atoms, the corresponding lower electronic charge density on the ortho and para carbons of the phenyl group (from 0.13–0.14 to 0.09–0.10), and finally the planar position of the phenyl ring, whose deviation from coplanarity is now only 4 degrees. The ortho effect suggested by some authors [20] is thus confirmed.

3.2. ENERGETICS OF PROTON TRANSFER

As discussed in the introduction, the spectral behaviour of 3-HF suggests that proton transfer occurs very quickly, but, in our opinion, many questions remain open:

- Are the two isomeric forms really related to stable equilibrium points of the excited-state potential energy hypersurface, or is the normal form simply an unstable intermediate?
- Is the temperature dependence, observed both in steady state and time resolved spectra, to be attributed solely to the effects of H-bonding impurities, hindering proton motion, or do vibrational normal modes also play an important role in the proton transfer kinetics?

Finally, if the latter assumption holds:

- Is the torsion of the phenyl group the only normal mode enhancing the ESIPT rate, or are other low frequency vibrations also important?

Answering the above questions requires a study of the dynamical properties of ESIPT; therefore, the quasi-stationary states associated with the two "initial" and "final" equilibrium positions of the hydrogen atom and their couplings must be determined. This requires knowledge of the potential energy surface, whose computation is not an easy task. In principle, the Born–Oppenheimer potential energy (PE) surface for an N-atom system depends on $3N-6$ independent coordinates; the possibility of mapping out the potential energy surface considering the whole set of independent coordinates is, of course, ruled out by the present state of the art. Therefore, the first problem to be faced is the choice of a suitable path across the potential energy surface, joining the two minima, which is usually called the reaction path. In general, the reaction path can be identified with a large amplitude local mode, the remaining $3N-7$ degrees of freedom may be considered only weakly coupled to it following adiabatically the motion of the reaction coordinates, so that this approximation reduces the potential energy requirements to an essentially one-dimensional calculation. The choice of the reaction path is not, of course, unique and should be dictated by chemical reasons. The usual recipe of defining the intrinsic reaction path (IRC) [49] consists in locating the transition state and then in following the steepest descent path in mass weighted Cartesian coordinates, leading to the products in the forward direction and to the reactants in the backward direction, is not always a safe procedure. There are many situations in which the IRC is not

adequate, one of these being the transfer of a light atom between two heavy atoms [50–52]. In these cases, there are at least two degrees of freedom with a large amplitude motion which must be explicitly included in the dynamical treatment of the system, namely the motions of the hydrogen atom and of the donor and acceptor heavy atoms. In the IRC approximation, one has to map out the whole potential energy surface for both degrees of freedom independently, optimizing for each point the geometry of the rest of the molecule. Apart from computational difficulties, which are particularly severe for the system under study since the mapping of the PE surface must be done for excited state, another question remains open:

- Is the intrinsic reaction path, built up taking into account one or more degrees of freedom, the most probable one?

The IRC presupposes that for every value of the reaction coordinate, the rest of the molecule has time enough to rearrange its geometry in a way which corresponds to the minimum energy configuration. Such a quasi-adiabatic path, involving the motion of several heavy atoms, might turn out to be slower than the slowest molecular vibration, which is not necessarily acceptable even as an approximate assumption; in other words, the formation of the product may be faster than the nuclear rearrangement of the rest of the molecule to the minimum energy configuration. Thus, expecially for the system under study, where experiments show beyond doubt that the process is extremely fast, a minimum energy path like the IRC might be meaningless. This point has been discussed by Shida et al. [52]; these authors have compared the velocity of proton transfer in malonaldehyde, the simplest model system for intramolecular proton transfer isomerization, using two different reaction paths: The MEP, the minimum energy path, and a path they call EVP, the expectation value path, constructed by considering the "average most probable" nuclear positions for each point of the reaction coordinate. Results show that although the MEP is associated to a significant lower barrier, the isomerization process may be faster along the EVP, since tunneling is much more effective for two reasons: (i) the PE profile is narrower, with a shorter distance between the two minima; (ii) the EVP does not require large displacements of the heavy atoms from their equilibrium positions, thus resulting in a less massive motion.

In the light of the above considerations, we have started the computation of the PE profile for the excited state proton transfer with the tentative assumption that the formation of the tautomeric form takes a shorter time than is required for the molecule to rearrange its nuclear configuration for each proton position. This assumption corresponds to a "frozen geometry" (FG) path, along which the proton jumps from one equilibrium site to the other without requiring any motion of the rest of the molecule.

The computed PE profile for FG proton transfer along a path joining directly the two minima is reported in fig. 6. The PE profile has a double well character, with a very high barrier of 2.147 eV (49.5 kcal/mol). The tautomer appears to have a higher energy than the normal form, but this is an artifact due to FG. In

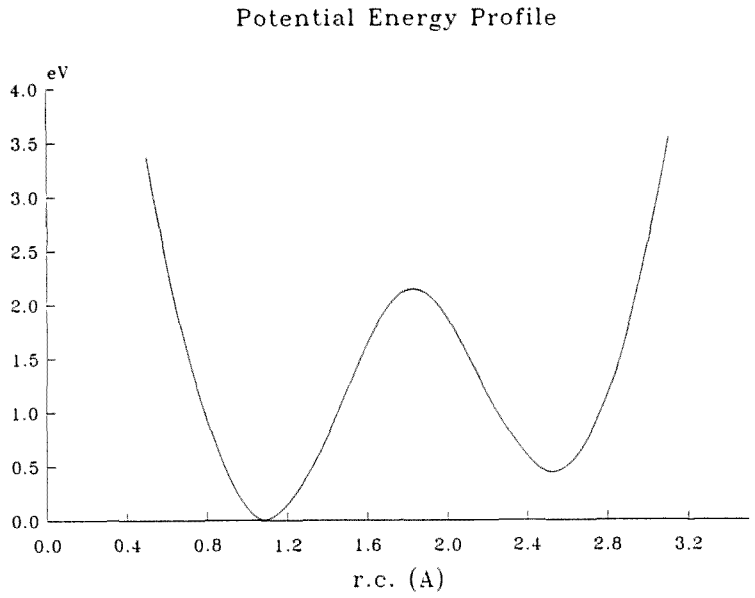

Fig. 6. Frozen geometry potential energy profile for proton transfer along the path joining directly the two minima.

fact, when the C–O bond distances are properly allowed to relax, the tautomer is stabilized with respect to the normal form of approximately 0.5 eV (11.5 kcal/mol). The height of the PE barrier, together with a large distance between the two minima, would result in a very long transition time, in complete disagreement with experimental suggestions. Therefore, we have also computed the PE profile for a simplified IRC. Due to computational difficulties, it has not been possible to locate a real transition state, since the computation of a Hessian matrix would take too long and, moreover, there would be no grounds for assessing its reliability. Therefore, we have confined ourselves to a simple mapping of the potential energy surface, taking the proton coordinates as the reaction coordinates and optimizing the geometrical parameters involving the oxygen atoms, i.e. bond distances and valence angles. In order not to complicate the matter, the torsional angle of the phenyl group which, as suggested by many authors, could be important in lowering the barrier height, has been kept constant and its role in the mechanism of proton transfer has been analyzed independently. The results show that phenyl torsion has very little influence on the barrier to proton transfer, so that this effect may be neglected. The energy barrier resulting from the simplified minimum energy path (MEP) is lowered to approximately half the value corresponding to the frozen geometry path, its value being 1.22 eV (28.2 kcal/mol).

The simplified MEP is shown in scheme 4. As expected, it is characterized by large contributions of the C–O and O–O stretching motions. The "pseudo" transition state, namely the structure which in our computation corresponds to a

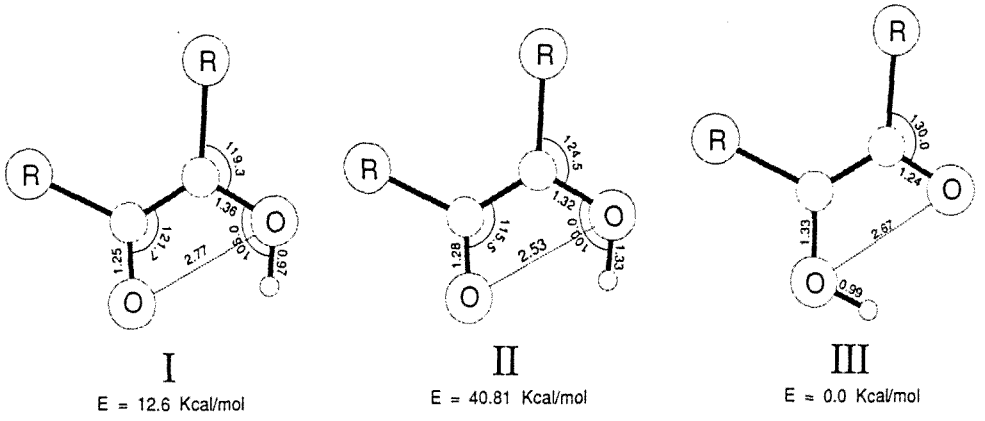

Scheme 4.

maximum of the PE profile, does not have a symmetric structure with the hydrogen atoms equally spaced between the two oxygens, but corresponds to a situation where the preexisting O–H bond is only partially broken.

The aims of this computation were twofold. Firstly, we intended to make sure that two stable minima separated by an energy barrier really characterize the H-bond under study, so that ESIPT cannot be considered as a result of a simple molecular relaxation to the vibrational ground state. Secondly, the knowledge of the saddle point structure may give useful information on the possibility that a particular vibrational mode can promote the ESIPT process. Indeed, the particular asymmetric structure of the saddle point indicates that a large amplitude C–C–O bending vibration, implying a sensible shortening of the O–O separation distance, could favour the hydrogen transfer to the tautomeric position, bringing it around the top of the barrier. Actually, such a mode does really exist, at least in the ground electronic state, for which we have performed a qualitative vibrational analysis at MNDO level. The computed vibrational frequencies for the electronic ground state normal form of 3-HF are shown in table 1, together with tentative assignments. The more suitable normal mode, falling at a frequency of 367 cm^{-1}, is sketched in fig. 7. It consists essentially of the two C–C–O bending local modes. We will continue making the assumption that in going to excited states the normal modes retain their forms and approximately their frequencies.

The root mean square (rms) amplitude of this normal mode is 0.21 Å. When quanta are added to such a mode, the potential role of the rms vibrational amplitude should be enhanced, although excitation increases the average O–O distance, because of the anharmonicity of the potential. In order to take into proper account the potential promoting effects of such a vibration, one should numerically solve the Schrödinger equation in a two-dimensional space [53]. This goes beyond the scope of this study, for we are only interested in estimating the isomerization rate. We have then simulated the promoting effect of the low frequency vibrational mode in

Table 1

Uncorrected AM1 vibrational frequencies of the ground-state normal form of 3-HF.

Frequency [cm^{-1}]	Assignments	Frequency [cm^{-1}]	Assignments
3384	O–H stretching	1320	
		1293	
3201		1244	
3200		1202	
3193		1197	C–C–H bending
3192	C–H stretching	1186	
3188		1179	
3184		1173	
3182		1156	
3180			
3167		1092	
		1008	
2029	C=O stretching	1006	C–C–H out of
		990	plane bending
1888	C=C stretching	982	
		962	
1780		921	
1775		891	
1770		813	
1760			
1640		828 492	
1563	In plane C–C–C ring modes	794 435	
1445		703 327	C–C–C out of
1386		692 306	plane and torsional
1376		668 286	mode
1221		656 247	
980		591 189	
741		127	
622			
		382	
1650	C–O stretching	373	
		367	O–C–C–O in
1630		266	plane bending
1489		74	
1467			
1338	C–C–O in plane mode	474	
941		469	
825		99	not assignable
549		54	
		33	
1590	C–O–H bending		
1515			

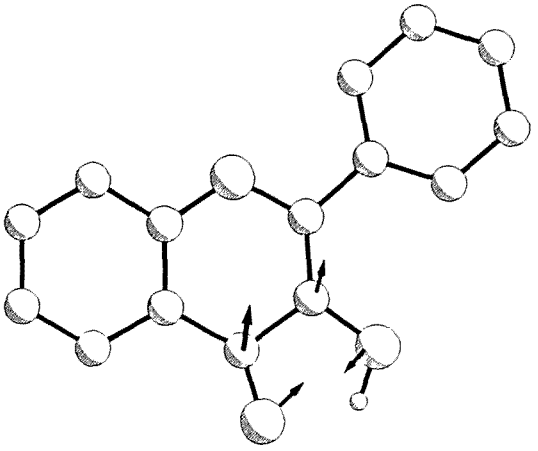

Fig. 7. Schematic plot of the low-frequency bending mode oscillating at 367 cm^{-1}.

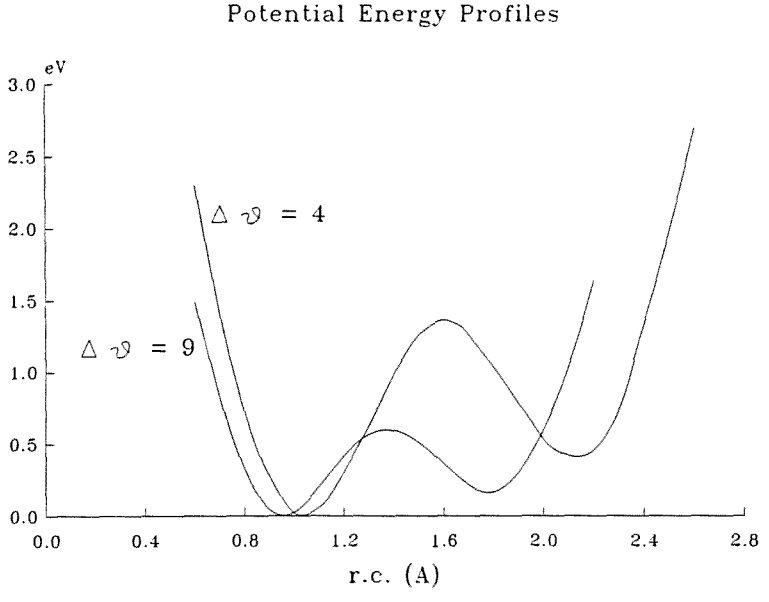

Fig. 8. Frozen geometry potential energy profile for $\delta\Theta = 4$ and 9 degrees.

a very simple way. We have computed the FG potential energy profiles for two O–O separation distances different from the equilibrium one; one PE profile computation has been performed for a C–C–O angle 4 degrees smaller than its equilibrium value ($\delta\Theta = 4$), corresponding to a shortening effect due to room

temperature amplitude of the bending vibration, the second PE profile has been computed for a $\delta\Theta$ of 9 degrees, corresponding to the most stretched position of a higher excited state. The two PE profiles are shown in fig. 8. In the first case, for proton transfer taking place from the highest displaced O–O separation, which classically corresponds to the zero kinetic energy point, the barrier height decreases to 1.37 eV (31.6 kcal/mol), while the distance between the two minima is reduced to 1.12 Å. In the second case, the barrier height is only 0.63 eV (14.6 kcal/mol), the distance between the two minima being only 0.83 Å.

4. Dynamics of the ESIPT process

4.1. TIME-DEPENDENT THEORY OF QUASI-STATIONARY STATES

For the sake of completeness, we briefly review the theory, referring the interested reader to refs. [54,55] for details and applications.

In terms of quantum mechanics, the ESIPT process is interpreted as meaning that 3-HF has been prepared in one of its possible quantum states of the normal form $\{|n\rangle^{N}\}$ and is observed, after a certain time, in one of the quantum states associated to the tautomer $\{|n\rangle^{T}\}$. The words "prepared", "observed" and "associated" would demand some comments (cf. refs. [31,32] or a fundamental text of quantum mechanics); here, we only remark that due to the preparation and observation, the states in question are not the usual stationary states of the isolated system, but depend on the ways they are prepared and observed. Since neither type of states is stationary, quantum mechanics establishes that there is a certain probability for the system prepared at $t = 0$ in one of the states of the manifold $\{|n\rangle^{N}\}$, $|k\rangle$, to be found at $t = t_1$ in one of the manifold $\{|n\rangle^{T}\}$, $|l\rangle$. That probability is the well-known Born probability, which for an orthonormal set is simply:

$$|\langle l \mid k(t_1)\rangle|^2. \tag{1}$$

Let us consider the Born probability for the decay of a quantum state $|j\rangle$ into a manifold $|M\rangle \equiv \{|m\rangle\}$. Assuming that $|j\rangle$ can only decay into states $|m\rangle$ and that the manifold $|M\rangle$ has only discrete states, it can be shown that the probability $p_{j\to M}$ can be represented as a Fourier sum [56]:

$$P_{j\to M}(t) = \sum_{u,v} R_{u,v}(0)\cos(\Omega_{u,v}(t), \tag{2}$$

where $R_{u,v}(0)$ and $\Omega_{u,v}$ are

$$R_{u,v}(0) = \{\tfrac{1}{2}\mathbf{T}^{+}(\mathbf{S}^{1/2}\mathbf{P}^{0}\mathbf{S}^{-1/2} + \mathbf{S}^{-1/2}\mathbf{P}^{0}\mathbf{S}^{1/2})\mathbf{T} \times \tfrac{1}{2}\mathbf{T}^{+}(\mathbf{S}^{1/2}\mathbf{P}\,\mathbf{S}^{-1/2} + \mathbf{S}^{-1/2}\mathbf{P}\,\mathbf{S}^{1/2})\mathbf{T}\}_{u,v} \tag{3}$$

and

$$\Omega_{u,v} = \varepsilon_{u,u} - \varepsilon_{v,v}. \tag{4}$$

The symbol $\varepsilon_{i,i}$ stands for the energy eigenvalue of state i, **T** is the unitary matrix that diagonalizes the Hamiltonian matrix, **S** is the overlap matrix, $\mathbf{P}^0$ is the matrix whose (k, k)th element is the probability that the given system is in the state $|k\rangle$ at $t = 0$, **P** is the projection matrix whose (j, j)th element is 1 if $|j\rangle$ is one of the final states of interest, 0 otherwise.

Expression (2) yields the ideal probability that a transition $j \rightarrow M$ occurs at time t_1; the experimental counterpart of the above quantity is the result of an observation, which usually takes time. Therefore, the observation will perform an average on the ideal probability of eq. (2), the actual probability of observing the transition at time t_1 is:

$$\langle P_{j\rightarrow M} \rangle = 1/2\sigma \int_{t_1-\sigma}^{t_1+\sigma} P_{j\rightarrow M}(t')\,\mathrm{d}t', \tag{5}$$

where σ is the time interval required by the measuring apparatus. The required time average involves an integral of the form:

$$I_{u,v} = 1/2\sigma \int_{t_1-\sigma}^{t_1+\sigma} \cos(\Omega_{u,v}t')\,\mathrm{d}t' = \cos(\Omega_{u,v}t)g(2\pi\sigma/T_{u,v}), \tag{6}$$

where

$$g(x) = \sin(x)/x; \quad T_{u,v} = 2\pi/\Omega_{u,v}. \tag{7}$$

Moreover, the quantum mechanical uncertainty affects the phase of the observed signal, since also the instant at which the initial state was prepared is not sharply defined. Therefore, a further averaging of eq. (2) is necessary. If we assume that the averaging is done on the same time interval $[t - \sigma, t + \sigma]$, we finally obtain:

$$\langle R_{u,v} \rangle = R_{u,v}(0)[g(\sigma/\Omega_{u,v})]^2. \tag{8}$$

Substitution of $\langle R_{u,v} \rangle$ for $R_{u,v}(0)$ in expression (2) gives the required transition probabilities.

Equation (2) defines the single-molecule Born transition probability, which is not the observable quantity under ordinary conditions. Let us extend the treatment to an ensemble of $N_{j,0}$ molecules, all prepared at $t = 0$ in the initial state $|j\rangle$, but observed at different times. We wish to know the average number $N_j(t)$ of molecules still found in the original state $|j\rangle$ at time t. In answer to this question we must consider the observation process, which in the specific case of 3-HF can be considered as a decay to a lower vibrational state, followed by the emission of the tautomeric

form. Under the assumption of complete incoherence, observation may be attributed two effects:

(i) it removes a number of molecules proportional to the Born probability;

(ii) it localizes the remaining molecules (those that are not subjected to the transition) in the original state.

An expression for $N_j(t)$ can then be found using an idealized scheme where the observation process is repeated at equal time intervals s:

$$N_j(t) = N_j(0)[1 - P_{j\to M}(s) \times s]^{t/s} \approx N_j(0)\mathrm{e}^{-p(s)t}, \tag{9}$$

where

$$P_{j\to M} = p_{j\to M}/s.$$

In obtaining eq. (9), we have made use of the relation

$$\lim_{s\to 0}(1 - xs)^{1/s} = \mathrm{e}^{-x}.$$

Equation (9) can be considered as a decay curve, so that $1/p(s)$ may be interpreted as the lifetime of the starting state.

4.2. THE REFERENCE PHYSICAL PROCESS

In terms of quantum mechanics, the process under study can be described as follows. A laser pulse excites the 3-HF molecule to one of the vibrational states of the first excited singlet (I^*). The photo-excitation may be regarded as a perturbation which prepares the system in a well-defined vibronic state. Therefore, the initial states have to be thought of as states that are stationary under the perturbation (i.e. the preparation procedure) and begin to change as the perturbation is switched off in a manner dependent on the way in which the switching off takes place [57]. If the latter is fast enough, the system is practically left in the quasi-stationary state corresponding to one of the possible vibrational states, say $|n\rangle^{\mathrm{N}}$, of I^*. The state $|n\rangle^{\mathrm{N}}$ begins to evolve and, since it is coupled to states of the tautomeric form having energies close to its own, there is a certain probability of finding it in the mth vibrational state of the excited tautomeric singlet (II^*), $|m\rangle^{\mathrm{T}}$. Subsequently, the state $|m\rangle^{\mathrm{T}}$ will decay very rapidly into the lowest energy states of its manifold, so that the whole process is not spontaneously reversible. The decay process may be more complicated if, in addition to internal conversion, other channels are open. We shall not take this possibility into account here.

4.3. DETERMINATION OF THE VIBRATIONAL STATE

The time evolution formalism between discrete states just reviewed has been applied to the three PE profiles of section 3 to compute transition probabilities and lifetimes of the photo-excited state of 3-HF.

The vibrational states associated to the two forms have been determined variationally using a basis set consisting of harmonic oscillator states centered at the minima of the two wells. Numerical techniques [58] have been preferred to analytical ones [59] for the computation of the Hamiltonian matrix. The computed energies of the lower vibrational states for the three different PE profiles are reported in table 2.

Table 2

Energy values of the vibrational states lying below the barrier for the three PE profiles discussed in the text (atomic units).

Profile $\delta\Theta$	Left-hand well	Right-hand well
	0.0738	0.0706
	0.0633	0.0607
	0.0523	0.0503
0°	0.0408	0.0399
	0.0291	0.0296
	0.0174	0.0196
	0.0057	
	0.0415	0.0386
	0.0304	0.0286
4°	0.0184	0.0187
	0.0062	
	0.0236	0.0187
9°	0.0159	0.0102
	0.0056	

For each PE profile, we have computed the single-molecule transition probability and the lifetime of the normal excited molecule taking into account only the states lying below the barrier (table 2), which can be easily assigned to one of the two equilibrium forms. We have not considered vibrational states with energies higher than the barrier, because the radiative transition probabilities from the ground state to each of them are affected by small Franck–Condon factors. Lifetimes corresponding to different transitions for each of the three PE profiles are reported in table 3.

For the first profile, corresponding to the longest O–O distance, the lifetime of the excited molecule in the normal form is 2244 ps for the transition $|3\rangle^N \rightarrow \{|1\rangle^T, |2\rangle^T\}$ and decreases to 3.14 ps for the transition $|7\rangle^N \rightarrow \{|1\rangle^T, \ldots, |6\rangle^T\}$.

The second profile, the intermediate one, gives a lifetime of 3.42 ps for the transition $|3\rangle^N \rightarrow \{|1\rangle^T, |2\rangle^T\}$, while transition $|4\rangle^N \rightarrow \{|1\rangle^T, |2\rangle^T, |3\rangle^T\}$ is characterized by a lifetime of 0.31 ps (fig. 9).

Table 3

Lifetimes of vibrational states of normal form at different values of $\delta\Theta$.

Profile $\delta\Theta$	Transition		Lifetime [ps]
	Initial state	Final states	
0°	$\|3\rangle$	$\{\|1\rangle, \|2\rangle\}$	2244
	$\|4\rangle$	$\{\|1\rangle, \|2\rangle, \|3\rangle\}$	144
	$\|5\rangle$	$\{\|1\rangle, \ldots, \|4\rangle\}$	25.4
	$\|6\rangle$	$\{\|1\rangle, \ldots, \|5\rangle\}$	12.5
	$\|7\rangle$	$\{\|1\rangle, \ldots, \|6\rangle\}$	3.14
4°	$\|2\rangle$	$\|1\rangle$	840
	$\|3\rangle$	$\{\|1\rangle, \|2\rangle\}$	3.42
	$\|4\rangle$	$\{\|1\rangle, \|2\rangle, \|3\rangle\}$	0.31
9°	$\|2\rangle$	$\{\|1\rangle, \|2\rangle\}$	0.43
	$\|3\rangle$	$\{\|1\rangle, \|2\rangle\}$	0.072

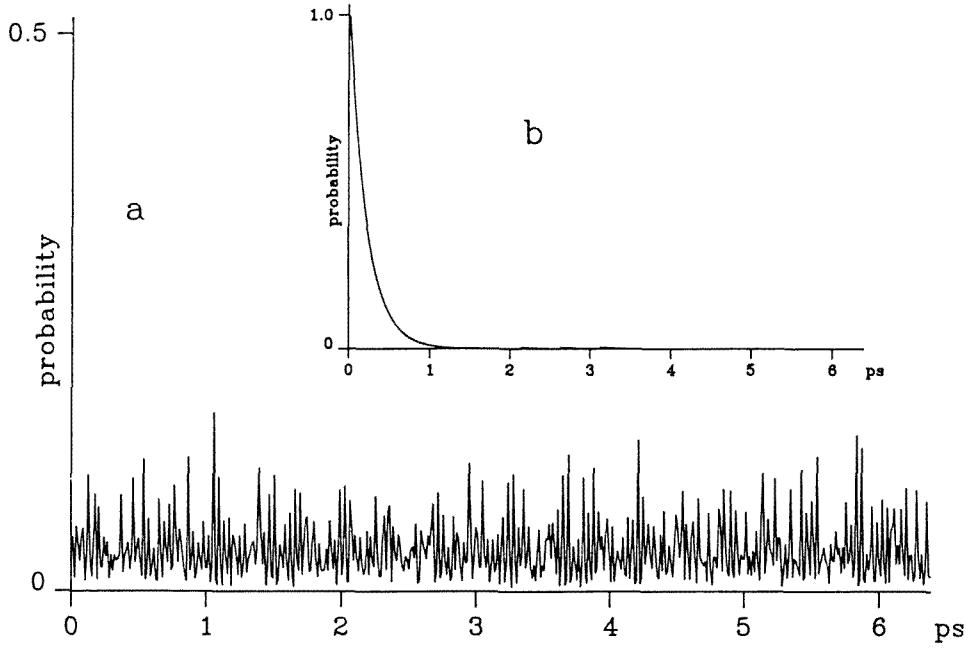

Fig. 9. Transition probability (a) and decay curve (b) for the transition $|4\rangle^N \rightarrow \{|1\rangle^T, \ldots, |3\rangle^T\}$. The energy profile is shown in fig. 8.

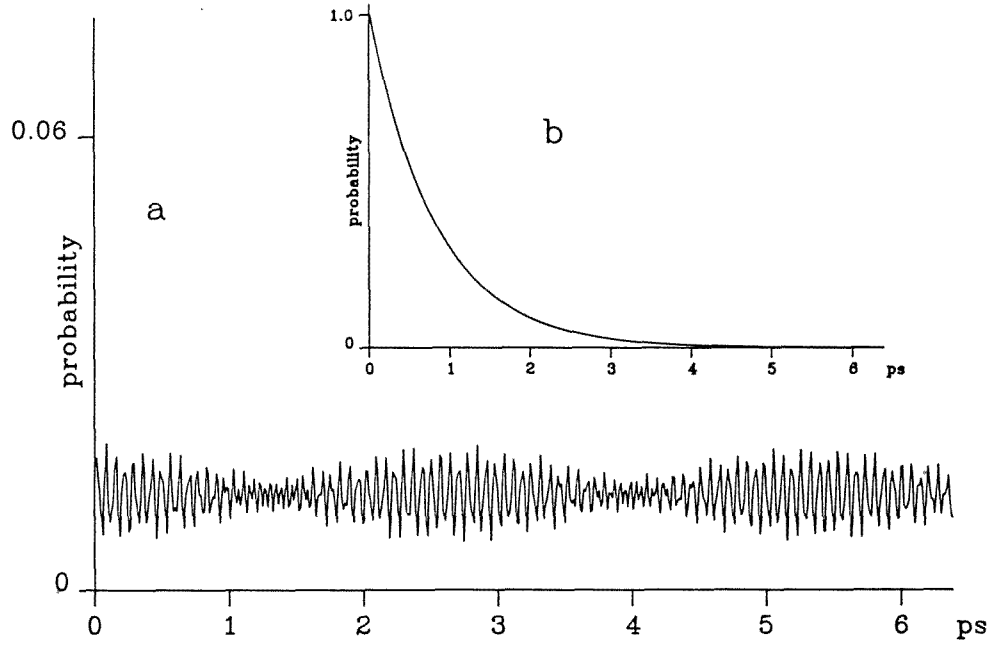

Fig. 10. Transition probability (a) and decay curve (b) for the transition $|2\rangle^N \rightarrow |1\rangle^T$. The energy profile is shown in fig. 8.

For the third profile, corresponding to the shortest O–O distance, we have considered only the $|2\rangle^N \rightarrow |1\rangle^T$ transition, which yields a lifetime of 0.4291 ps (fig. 10). We have found a very short lifetime of 0.072 ps for the transition $|3\rangle^N \rightarrow \{|1\rangle^T, |2\rangle^T\}$, where the energy of $|3\rangle^N$ is only slightly higher than the barrier ($\delta E = 0.0004$ Hartree) and so the state can still be considered localized in the left-hand well (cf. table 2 and fig. 10). These results show that the lifetime of I^* depends strongly on the O–O distances; a lifetime of the same order of magnitude as the experimental one is obtained when the shortening effect of the bending low-frequency normal mode is taken into account. Alternatively, a fast decay time of I^* requires the assumption that higher O–H vibrational states are populated by photoexcitation. The following mechanism for proton transfer can be suggested:

- The laser pulse prepares the molecule in an excited vibrational state of I^*; some vibrational quanta are added to the O–O bending vibration and this produces a periodic, sensible shortening of the O–O distance.
- When this distance is quite short, the probability of a transition of the proton is very high, even though the O–H vibration is in one of the lower excited states. Then a vibrational-state transition occurs from the form I^* to the form II^* and the system ends up in one of the vibrational levels of the tautomeric form. This transition involves proton transfer, because the proton is now found to be in the right-hand well of figs. 6 and 8.

- The proton is blocked in the tautomeric form by a vibrational cascade to lower vibrational states, which makes the reverse proton transfer unlikely. Finally, the radiative decay to the electronic ground state with the characteristic emission occurs.

5. Conclusions

The results presented above make possible a better understanding of the structural features which determine the spectral behaviour of 3-HF. We summarize them, following the scheme outlined above.

Computations suggest that ESIPT arises from the breaking of the C–C double bond nearest to the hydroxyl group upon excitation; proton transfer occurs so as to minimize the antibonding interactions arising from photoexcitation of an electron to the LUMO level of the normal form.

The existence in the excited state of two stabe isomeric forms is confirmed by our computation, which predicts, for the two proton positions, two deep minima separated by a high barrier.

The rapidity of ESIPT is modelled in terms of a promoting effect of a low-frequency bending mode, bringing the donor and acceptor group to a shorter distance; such a mode is probably excited in a high-energy state by a laser pulse, since the nuclear coordinates of the atoms involved change upon excitation. Similar models have recently been suggested [60].

The torsional mode of the phenyl ring appears to have little effect on proton dynamics. The coplanar position of the phenyl group is an important factor is stabilizing the tautomeric form but, as is also suggested by experiments [61], its relaxation probably follows proton motion rather than promotes it, as suggested by the scarce effect it has on the energy barrier to proton switching.

The temperature dependence of the steady state and time resolved spectra may then be ascribed not only to the formation of an H-bond complex, which at very low temperatures is prevented by the low mobility of solvent molecules, but also to the Boltzmann population of the low-frequency bending mode.

Finally, solvent effects may be modelled as follows: when both oxygens are involved in two or more intermolecular H-bonds, the promoting effect of the bending vibration is weaker, since the amplitude of the motion shortening the O–O distance will be smaller; therefore, the molecule is essentially incapable of changing its initial form. On the other hand, when only one intermolecular H-bond is formed, it may act as a bridge for proton transfer, favouring the switching to the tautomeric configuration.

Acknowledgements

The authors thank Dr. Renato Contillo for bringing the problem to their attention and for many useful discussions. The support of CNR and MURST is acknowledged.

References

[1] S. Voelker, R.M. MacFarlane, A.Z. Genack, H.P. Trommsdorff and J.H. van der Waals, J. Chem. Phys. 67(1977)1759;
J. Goodman and L.E. Brus, J. Amer. Chem. Soc. 100(1978)7472.
[2] K. Peters, M.L. Applebury and P.M. Rentzepis, Proc. Nat. Acad. Sci. USA 74(1977)3119.
[3] A. Weller, Naturwissenschaften 42(1955)175.
[4] P.F. Barbara, P.K. Walsh and L.E. Brus, J. Phys. Chem. 93(1989)29.
[5] P.F. Barbara, L.E. Brus and P.M. Rentzepis, J. Amer. Chem. Soc. 102(1981)5631;
T. Elsaesser and W. Kaiser, Chem. Phys. Lett. 128(1986)231.
[6] J. Goodman and L.E. Brus, J. Amer. Chem. Soc. 100(1978)7472;
K.K. Smith and K.J. Kaufman, J. Phys. Chem. 82(1978)2286.
[7] A. Mordzinski and W. Kuhle, J. Phys. Chem. 90(1986)1455;
N.P. Ernsting, J. Phys. Chem. 89(1985)4832;
N.P. Ernsting, A. Mordzinski and B. Dick, J. Phys. Chem. 91(1987)1404.
[8] T. Nishiya, S. Yamauchi, N. Hirota, M. Baba and I. Hanazaki, J. Phys. Chem. 90(1986)5730.
[9] S. Nagaoka, U. Nagashima, N. Ohta, M. Fujita and T. Takemura, J. Phys. Chem. 92(1988)166.
[10] M.H. Van Benthen and G.D. Gillispie, J. Phys. Chem. 88(1984)2954;
M.H. Van Benthen, G.D. Gillispie and R.C. Haddom, J. Phys. Chem. 86(1982)4281;
G. Smulevich and P. Foggi, J. Chem. Phys. 87(1987)5657.
[11] J.F. Ireland and P.A.H. Wyatt, Adv. Phys. Org. Chem. 12(1976)131;
E. Vander Donckt, Prog. React. Kinet. 5(1979(273.
[12] H.J. Heller and H.R. Blattmann, J. Pure Appl. Chem. 36(1973)141.
[13] P. Chou, D. McMorrow, T.J. Aartsma and M. Kasha, J. Phys. Chem. 88(1984)4596.
[14] M.M. Caldwell, R. Robberecht and S.D. Flint, Plant 58(1983)445;
M.S. Darling, Amer. J. Bot. 76(1989)1698.
[15] P.K. Sengupta and M. Kasha, Chem. Phys. Lett. 68(1979)382.
[16] G.J. Woolfe and P.J. Thistlethwaite, J. Amer. Chem. Soc. 103(1981)6916.
[17] D. McMorrow and M. Kasha, J. Amer. Chem. Soc. 105(1983)5133.
[18] D. McMorrow and M. Kasha, Proc. Nat. Acad. Sci. USA 81(1984)3375.
[19] D. McMorrow and M. Kasha, J. Phys. Chem. 88(1984)2235.
[20] A.J.G. Strandjord, D.E. Smith and P.F. Barbara, J. Phys. Chem. 89(1985)2362.
[21] B.L. Shaw and T.H. Simpson, J. Chem. Soc. 655(1955).
[22] C.I. Jose, P.S. Phadke and A.V. Rama Rao, Spectrochim. Acta Part A, 30A(1974)1199.
[23] M. Itoh, K. Takumura, Y. Tanimoto, Y. Okada, H. Takeuchi, K. Obi and I. Tanaka, J. Amer. Chem. Soc. 104(1982)4146;
M. Itoh, Y. Fujiwara, M. Sumitani and K. Yoshihara, J. Phys. Chem. 90(1986)5672.
[24] A.J.G. Strandjord and P.F. Barbara, Chem. Phys. Lett. 98(1983)21.
[25] A.J.G. Strandjord, J.H. Courtney, D.M. Fridrich and P.F. Barbara, J. Phys. Chem. 87(1983)1125.
[26] D. McMorrow, T.P. Dzugan and T.J. Aartsma, Chem. Phys. Lett. 103(1984)492.
[27] G.A. Brucker and D.F. Kelley, J. Phys. Chem. 91(1987)2856.
[28] B. Dick and N.P. Ernsting, J. Phys. Chem. 91(1987)4261.
[29] S.L. Studer, P.T. Chou and D. McMorrow, Chem. Phys. Lett. 161(1989)361.
[30] G.A. Brucker and D.F. Kelley, J. Phys. Chem. 93(1989)5179.
[31] B. Dick, J. Phys. Chem. 94(1990)5752.
[32] T.D. Boumann, M.A. Knobeloch and S. Bohan, J. Phys. Chem. 89(1985)4460.
[33] M.J.S. Dewar and W. Thiel, J. Amer. Chem. Soc. 107(1977)1489.
[34] M.J.S. Dewar, E.G. Zoebisch, E.F. Healy and J.J.P. Stewart, J. Amer. Chem. Soc. 107(1985)3902.
[35] M.J.S. Dewar, M.A. Fox, K.A. Campbell, C.C. Chen, J.B. Friedheim, M.K. Halloway, S.C. Kim, P.B. Lieschesky, A.M. Pakiari, T.P. Tien and E.G. Zoebisch, J. Comput. Chem. 5(1984)480.

[36] M. Seel and G. Del Re, Int. J. Quant. Chem. 30(1986)563.
[37] J. Troe and K.M. Weitzel, J. Chem. Phys. 88(1988)7030.
[38] M.J.S. Dewar and C. Boubleday, J. Amer. Chem. Soc. 100(1978)4935.
[39] H.E. Zimmermann and A.M. Weber, J. Amer. Chem. Soc. 111(1989)995.
[40] C. Rulliere, A. Declemy, P. Kottis and L. Ducasse, Chem. Phys. Lett. 117(1985)583.
[41] P. Ertl, Int. J. Quant. Chem. 38(1990)231;
P. Ertl, Coll. Czech. Chem. Comm. 54(1989)1433;
P. Ertl and J. Leska, J. Mol. Struct. (THEOCHEM) 165(1988)1.
[42] P. Ertl, Coll. Czech. Chem. Comm. 55(1990)1399.
[43] A.A. Voityiuk and A.A. Bliznyuk, Theor. Chim. Acta 72(1987)223; J. Mol. Struct. (THEOCHEM) 164(1988)343.
[44] E.L. Coitino, K. Irving, J. Rama, A. Iglesias, M. Paulino and O.N. Ventura, J. Mol. Struct. (THEOCHEM) 210(1990)405.
[45] V. Barone, private communication.
[46] J.J.P. Stewart, MOPAC 6.00: Q.C.P.E. No. 438.
[47] M.J.S. Dewar and D.A. Liotard, J. Mol. Struct. (THEOCHEM) 206(1990)123.
[48] G. Del Re, A. Peluso and C. Minichino, Can. J. Chem. 63(1985)1850.
[49] K. Fukui, J. Phys. Chem. 74(1970)4161; Accts. Chem. Res. 14(1981)368;
R.A. Marcus, J. Chem. Phys. 45(1966)4493, 49(1968)2610.
[50] J.C.D. Brand and C.V.S. Ramachadrea Rao, J. Mol. Spectros. 61(1976)360.
[51] T. Carrington, Jr. and W.H. Miller, J. Chem. Phys. 81(1984)3942, 84(1986)4364.
[52] N. Shida, P.F. Barbara and J.E. Almlof, J. Chem. Phys. 91(1989)4061.
[53] N. Sato and S. Iwata, J. Chem. Phys. 89(1988)2932.
[54] G. Del Re, W. Förner, D. Hofmann and J. Ladik, J. Chem. Phys. 139(1989)265.
[55] G. Del Re and C. Adamo, J. Phys. Chem. 95(1991)4231.
[56] G.G. Hall and H. Nobutoki, Theor. Chim. Acta 74(1988)23.
[57] A. Messiah, *Quantum Mechanics*, 11th ed. (North-Holland, Amsterdam, 1985).
[58] M. Abramowitz and I.A. Stegun (eds.), *Handbook of Mathematical Functions* (Dover, New York, 1972).
[59] J. Brickmann and H. Zimmermann, J. Chem. Phys. 50(1969)1608.
[60] G.A. Brucker, T.C. Swinney and D.F. Kelley, J. Phys. Chem. 95(1991)3190.
[61] G.A. Brucker and D.F. Kelley, J. Phys. Chem. 92(1988)3805.